Transactions of A. Razmadze
Mathematical Institute
Vol. **179** (2025), issue 2, 247–255

APPLICATION OF A PROBABILISTIC-STATISTICAL METHODS OF SCATTERED RADIO WAVES IN TURBULENT PLASMA

GIORGI JANDIERI[1], ZAZA SANIKIDZE[2*] AND NINO MCHEDLISHVILI[3]

Abstract. The scintillation effects in a randomly varying equatorial terrestrial ionosphere are investigated for the first time. Second order statistical moments of the phase fluctuations of scattered ordinary and extraordinary radio waves in the turbulent alongatingconductive collision ionospheric magnetized (COCOIMA) plasma are calculated by using a probabilistic-statistical method containing complex geometrical optics approximation and a smooth perturbation method considering the diffraction effects. Polarization coefficients of these waves in the equatorial ionosphere are obtained for the first time. The scintillation level includes the variance and the correlation functions of scattered radio waves (RW). Statistical characteristics contain: complex refractive index, anisotropy factor characterizing elongated electron density irregularities, tilting angle of anisotropic plasmonic structures with respect to the geomagnetic lines of forces, complex permittivity components of the equatorial ionosphere including the Hall, Pedersen and longitudinal conductivities. Numerical calculations are carried out using the hybrid anisotropic correlation function of electron density fluctuations containing both exponential and power-law spectral functions having arbitrary spectral index, applying the experimental data. A new feature of the "Fountain Effect" in the equatorial ionosphere is revealed. The anisotropy parameters of electron density irregularities has an influence on the scintillation index of both the ordinary and extraordinary waves shifting maxima of S_4 curves in opposite sides at weak and moderate scintillations.

1. Introduction

The statistical characteristics of scattered RWs in a randomly inhomogeneous media are well studied [4, 5]. Ionospheric irregularities are the perturbations in electron density or total electron content (TEC) from a few meters to several tens of kilometers [3, 11]. The evolution of elongated plasmonic structures can be studied with a spatial fluctuation of TEC (SFT) maps containing the size, shape, orientation and intensity distribution of these inhomogeneities at lower latitudes. Several anisotropic structures are elongated mainly in the north-south direction. The geomagnetic field leads to the birefringence of RWs leading to the excitation of both ordinary (O-) and extraordinary (E-) waves. The error of the radio signal phase radiating by satellite radio navigation systems consists of the variance of the phase fluctuation of the radio signal, the variance of thermal noise and the variance of the generator's noise. Ionospheric scintillation leads to the enhancements and fading of the radio signals propagating in the night-time F-region at equatorial latitudes. Calculation of the statistical characteristics of RWs propagating in the equatorial ionosphere and investigation of scintillation phenomena will be widely used in the Global Navigation Satellite System (GNSS). The error of the phase of the navigation radio signal radiating by satellite radio navigation systems consists of the variance of the phase fluctuation of the radio signal, the variance of thermal noise and the variance of the generator's noise. Ionospheric scintillations are caused by a root-mean square deviation (RSD) of the electron concentration fluctuation in the ionosphere on the fluctuation of the phase of the navigation radio signal.

The scintillation phenomena of electromagnetic waves propagating in the polar ionosphere were considered in [6–8]. Statistical characteristics of scattered RWs in the equatorial ionosphere have been investigated in [9, 10]. The morphology of scintillations was described by the second order statistical moments of scattered RWs.

2020 *Mathematics Subject Classification.* 76F55, 60H15, 60J60.
Key words and phrases. Probabilistic-statistical methods; Turbulence; Random processes; Radio waves; Scattering.
*Corresponding author.

Ionospheric irregularities and scintillations of radio signals near the geomagnetic equator were observed [15] by three identical Swarm satellites. These studies are based on weak scintillation theory. Equatorial phase scintillations were used to obtain information on the power spectrum of the electron density irregularities that cause scintillations, as well as on the drift speed irregularities across the signal path. The linear scale of the irregularities causing scintillation can be determined directly from the basic dependence of the scintillation index.

Radar backscatter and AE-C satellite observations show that in low-latitude regions near the magnetic equator after midnight electron density, the irregularities in the topside ionosphere are the field-aligned plasma density depletion structures with sizes ranging from a few meters to several tens of kilometers. Statistical characteristics of the phase fluctuations and the equatorial scintillation phenomena are based upon rocket (bottomside) and satellite (topside) irregularity measurements (for example "plume-like" and wedge) and large-scale equatorial plasma bubbles (EPBs) [12, 15]. The detrended TEC with a specific window size is used to capture the characteristic depletion signatures, indicating the possible presence of the EPBs. The TEC depletions, amplitude and phase scintillation indices from multi-constellation GNSS signals were probed to verify the vulnerability of the signals towards the scintillation effects over the region.

For a sufficiently thin layer of irregularities, the amplitude fluctuations within the layer are negligible, while the phase variation on the incident radio wave is significant. The application of the Wentzel–Kramers–Brillouin method to the equatorial bubble is used to obtain the amplitude and phase variations on the ground. This theory allows one to investigate statistical peculiarities of irregularities such as mean square fluctuations of electron density and power spectra of the irregularities.

In Section 2 of this paper, we consider the signal statistics, that is, calculation of the root-mean square deviation (RSD) of the phase fluctuations by using the stochastic differential equation for a 2D spectral function of phase fluctuations taking into account diffraction effects. Polarization coefficients of O- and E- waves for the equatorial ionosphere are calculated for the first time. Second order statistical moments are obtained for an arbitrary correlation function of electron density fluctuations. Section 3 presents numerical calculations carried out for the "hybrid" mutual coherence function (MCF) of the complex phase of a radio signal received on the ground, using experimental data. The scintillation level is estimated for different anisotropy factors and the slope angle of elongated electron density irregularities with respect to the geomagnetic force lines. Conclusions are given in Section 4.

2. Methods

2.1. **Probabilistic-statistical method for calculating the corresponding characteristics of scattered radio waves in the equatorial ionosphere.** The electric field satisfies the wave equation:

$$(\nabla_i \nabla_j - \Delta\delta_{ij} - k_0^2 \tilde{\varepsilon}_{ij}) E_j(\mathbf{r}) = 0, \tag{2.1}$$

where $k_0 = \omega/c$ is the wavenumber of an incident wave with frequency ω; Δ is the Laplacian, δ_{ij} is the Kronecker symbol, $\tilde{\varepsilon}_{ij} = \varepsilon_{ij} - i\tilde{\sigma}_{ij}$ and $\tilde{\sigma}_{ij} \equiv \sigma_{ij}(4\pi/k_0 c)$ are the second rank tensors of, respecively, permittivity and conductivity of the COCOIMA plasma. The wave field is given by $E(\mathbf{r}) = E_0 \exp\{\Phi(\mathbf{r})\}$, where $\Phi(\mathbf{r})$ is the complex phase of the RW: $\Phi(\mathbf{r}) = \varphi_0 + \varphi_1 + \varphi_2 + \cdots$. The term, $\varphi_0 = ik_0 z + ik_\perp y$, corresponds to an incident wave, taking into account the diffraction effects, $k_\perp \ll k_0$; other terms are random functions of the spatial coordinates.

The normalized conductivity tensor $\tilde{\sigma} = 4\pi\hat{\sigma}/k_0 c$ of ionospheric plasma at equatorial latitude [2] contains the Hall σ_H, Pedersen $\sigma_\perp$ and longitudinal $\sigma_\parallel$ conductivities:

$$\sigma_H = e^2 n_e \left(\frac{\omega_e}{m_e(\nu_e^2 + \omega_e^2)} - \frac{\omega_i}{m_i(\nu_{in}^2 + \omega_i^2)} \right), \quad \sigma_\perp = e^2 n_e \left(\frac{\nu_e}{m_e(\nu_e^2 + \omega_e^2)} + \frac{\nu_i}{m_i(\nu_{in}^2 + \omega_i^2)} \right),$$
$$\sigma_\parallel = e^2 n_e \left(\frac{1}{m_e \nu_e} + \frac{1}{m_m \nu_{in}} \right),$$

where e and m_e are the charge and mass of an electron, $\nu_e = \nu_{en} + \nu_{in}$ is the effective collision frequency of electrons with other plasma particles; ω_e and ω_i are the angular gyrofrequencies of an electron and

ion, respectively; electron density $n_e(\mathbf{r})$ is a fluctuating term, $\nu_e = \nu_{en} + \nu_{in}$ is the effective collision frequency of electrons with ions and neutral particles

$$\nu_{ei} = N\left[59 + 4.18\log\left(\frac{T_e^3}{N}\right)\right] \times 10^{-6} T_e^{-3/2} \text{ [m.k.s]} \quad \text{and} \quad \nu_{en} = 5.4 \times 10^{-16} N_n T_e^{1/2} \text{ [m.k.s]}.$$

From equation (2.1), we obtain

$$\frac{\partial\psi}{\partial x} + \frac{i}{k_x(E_{0z}/E_{0x}) - 2k_0}\left[k_x(k_y + k_\perp)(E_{0y}/E_{0x}) + k_x k_0(E_{0z}/E_{0x}) - k_y(k_y + 2k_\perp)\right]\psi$$
$$= -i\frac{k_0^2}{k_x(E_{0z}/E_{0x}) - 2k_0}\left(\tilde{\varepsilon}_{xx}^{(1)} - i\tilde{\varepsilon}_{xz}^{(1)}\frac{E_{0z}}{E_{0x}}\right).$$

Here, ψ is the Fourier transform of Φ, or its fluctuations.

Let a homogeneous external magnetic field lie in the YOZ plane and the wave vector $\mathbf{k}$ be directed along the $Y-$axis, and let θ be an angle between these vectors. The components of the dielectric permittivity for the equatorial ionosphere can be written as follows:

$$\tilde{\varepsilon}_{xx} = \varepsilon_\perp - i\tilde{\sigma}_\perp, \quad \tilde{\varepsilon}_{xy} = i(æ + \tilde{\sigma}_H)\sin\theta, \quad \tilde{\varepsilon}_{xz} = i(æ + \tilde{\sigma}_H)\cos\theta, \quad \tilde{\varepsilon}_{yx} = -\tilde{\varepsilon}_{xy}, \quad \tilde{\varepsilon}_{zx} = -\tilde{\varepsilon}_{xz},$$
$$\tilde{\varepsilon}_{yy} = (\varepsilon_\perp + p_0 u\cos^2\theta) - i(\tilde{\sigma}_\parallel\cos^2\theta + \tilde{\sigma}_\perp\sin^2\theta), \quad \tilde{\varepsilon}_{yz} = -\left[p_0 u + i(\tilde{\sigma}_\perp - \tilde{\sigma}_\parallel)\right]\sin\theta\cos\theta,$$
$$\tilde{\varepsilon}_{zy} = \tilde{\varepsilon}_{yz}, \quad \tilde{\varepsilon}_{zz} = (\varepsilon_\perp + p_0 u\sin^2\theta) - i(\tilde{\sigma}_\parallel\sin^2\theta + \tilde{\sigma}_\perp\cos^2\theta),$$

where $\varepsilon_\perp = 1 - p_0$, $p_0 = \mathrm{v}/(1-u)$, $u = (eH_0/m_e c\ \omega)^2$ are the non-dimensional magneto-ionic parameters of the COCOIMA plasma, $\omega_p(\mathbf{r}) = \left[4\pi n_e(\mathbf{r})e^2/m_e\right]^{1/2}$ is the plasma frequency. They contain both regular and fluctuating terms (n_1).

The complex refractive index of the COCOIMA plasma in the conductive equatorial ionosphere can be written as $N^2 = \Gamma_0 + i\Gamma_1$ [9]; polarization coefficients of scattered RWs at $s \ll \varepsilon_{ij}, \tilde{\sigma}_{ij}$ are written in the form

$$P_{1,2} = \frac{\langle E_y\rangle}{\langle E_x\rangle} = P' - iP'', \quad G_{1,2} = \frac{\langle E_z\rangle}{\langle E_x\rangle} = -(G' + iG'').$$

The right part contains electron density fluctuations; the angular brackets denote an ensemble average, the indices 1 and 2 refer to O- and E- waves, respectively. Below, the indices in the polarization coefficients are omitted for brevity.

Taking into account the geometry of the task, for the polarization coefficients we obtain

$$P_{1,2} = \frac{(\Psi_1\Psi_3 - \Psi_2\Psi_4) - i(\Psi_2\Psi_3 + \Psi_1\Psi_4)}{\Psi_3^2 + \Psi_4^2}\sin\theta = P' - iP'',$$

where

$$\Psi_1 = (\sigma_\parallel - \sigma_\perp)(\Gamma_1 + \sigma_\perp) + p_0 u(\Gamma_0 - \varepsilon_\perp) - (æ + \sigma_H)^2, \quad \Psi_2 = (\sigma_\parallel - \sigma_\perp)(\Gamma_0 + \Gamma_1 - \varepsilon_\perp + \sigma_\perp),$$
$$\Psi_3 = (æ + \sigma_H)\left[(\sigma_\parallel - \sigma_\perp)\sin^2\theta + p_0 u\cos^2\theta + \varepsilon_\perp\right], \quad \Psi_4 = \varepsilon_\parallel(æ + \sigma_H).$$
$$G_{1,2} = -\frac{1}{F_1^2 + F_2^2}\left[(F_1F_3 + F_2F_4) + i(F_1F_4 - F_2F_3)\right] = -(G' + iG''),$$

where

$$F_1 = \Gamma_0 - (\varepsilon_\perp + p_0 u\sin^2\theta), \quad F_2 = \Gamma_1 + (\sigma_\parallel\sin^2\theta + \sigma_\perp\cos^2\theta),$$
$$F_3 = p_0 uP' - (\sigma_\parallel - \sigma_\perp)P'', \quad F_4 = (æ + \sigma_H)\cos\theta - P''p_0 u - P'(\sigma_\parallel - \sigma_\perp).$$

As a result, from equation (2.1) we obtain the stochastic differential equation

$$\frac{\partial\psi}{\partial x} + \frac{k_0}{4}(C_0 + iC_1)\psi = \frac{k_0}{4}(e_0 + ie_1)n_1, \tag{2.2}$$

where $C_0 = a_1b_0 - a_0b_1$, $C_1 = a_0b_0 + a_1b_1$, $a_0 = 2 + G'x$, $a_1 = G''x$, $b_0 = [G' - P'(y+\mu)]\,x + (y^2 + 2\mu y)$, $b_1 = [G'' + P''(y+\mu)]\,x$, $\mu = k_\perp/k_0$ is the diffraction parameter, $e_0 = a_1d_0 + a_0d_1 = 2d_1 + (G''d_0 + G'd_1)x = 2d_1 + \alpha_1 x$, $d_0 = \varepsilon_\perp - G'(æ + \sigma_H)\cos\theta$, $e_1 = a_0d_0 - a_1d_1 = 2d_0 + (G'd_0 - G''d_1)x = 2d_0 + \alpha_2 x$, $d_1 = \sigma_\perp + G''(æ + \sigma_H)\cos\theta$, $x = k_x/k_0$ and $y = k_y/k_0$ are nondimensional wave parameters.

Taking into account the boundary condition $\psi(k_x, k_y, L = 0) = 0$, from equation (2.2), for the phase fluctuations we obtain

$$\psi(k_x, k_y, L) = \frac{k_0}{4} \int\limits_0^L dz'(e_0 + ie_1)n_1(k_x, k_y, z') \exp\Big[-\frac{1}{4}(C_0 + iC_1)k_0(L - z')\Big].$$

The MCF of the phase fluctuation of a radio signal received on the ground and containing useful information about ionospheric irregularities looks as follows:

$$W_\varphi(\eta_x, \eta_y, L) = \pi k_0^4 L \int\limits_{-\infty}^{\infty} dx \int\limits_{-\infty}^{\infty} dy(e_0^2 + e_1^2)V_n(k_0x, k_0y, k_0\Lambda_0) \exp(-i\eta_x x - i\eta_y y). \tag{2.3}$$

Here: $\Lambda_0 = (h_0x^2 + h_1x + h_2)/4$, $h_0 = (G'^2 + G''^2) + (G''P'' - G'P')(y + \mu)$, $h_2 = 2(y^2 + 2\mu y)$, $h_1 = G'y^2 + 2(G'\mu - P')y + 2(G' - P'\mu)$, L is a distance the radio wave propagates in the ionosphere, $V_n(k_x, k_y, k_z)$ is an arbitrary correlation function of electron density fluctuations, η_x and η_y are small distances between observation points in the XOY plane.

Small-scale plasmonic structures (from hundreds of meters up to kilometers) mainly affect the amplitude scintillation of radio signals, while the large-scale irregularities contribute to phase fluctuations. The spatial correlation function (2.3) and the scintillation index S_4, describing an expected diffraction pattern on the ground are related to the phase auto-correlation function [7, 8]

$$S_4^2 = \int\limits_{-\infty}^{\infty} dx \int\limits_{-\infty}^{\infty} dy W_\varphi(x, y) - \int\limits_{-\infty}^{\infty} dx \int\limits_{-\infty}^{\infty} dy W_\varphi(x, y) \left[\cos(\Upsilon x^2)\cos(\Upsilon y^2) - \sin(\Upsilon x^2)\sin(\Upsilon y^2)\right].$$

Here: $\Upsilon = 2k_0^2/k_f^2$, $k_f = \sqrt{4\pi/\lambda z}$ is the Fresnel wavenumber, λ is the signal wavelength, z is the average height of a scattered layer. From this function it is possible to derive the experimental parameters of the scintillation phenomenon in the receiving plane.

3. Results

3.1. **Numerical calculations.** Numerical analyses are performed for an incident radio wave with a frequency of 40 MHz ($\lambda = 7.5\ m$). Plasma parameters at an altitude of 300 km : $u = 0.0012$, v = 0.0133; the Fresnel radius and Fresnel wavenumber are 1.5 km and 2.4 km^{-1}.

The full set of equatorial F propagation phenomena, namely, the occurrence of 3-m plume-like, wedge structures and VHF/GHz scintillations, was recorded. The height-integrated root-mean-square electron density deviation of ∼200-m scale irregularities causing 1.7-GHz scintillations maxima was determined in extended 3-m plume structures [12]. SFT with the GNSS Earth Observation Network of Japan (GEONET) is sensitive to small-scale ionospheric irregularities with horizontal scales of $\sim 15 - 90\ km$. In the equatorial ionosphere, the small-scale ionospheric irregularities range from a few meters to several tens of kilometers.

Measurements of signal parameters of a satellite moving in the ionosphere show that in the F-region of the ionosphere, irregularities have power-law spectrum with a spectral index p. It is associated with the irregularity power spectrum and can be determined from the power spectra of weak scintillations [14]. Most values of the spectral index, p, are in the range of 0.5 to 2.5. Magnetic field measurements using the High-Resolution Challenging Minisatellite Payload (CHAMP) show [1, 13] that the spectral indices were in the range of 1.4 to 2.6. The index interval $p = 2.0 - 2.2$ has been established by the Stretched Rohini Satellite Series (SROSSC2). Equatorial phase scintillations were used to obtain information on the power spectrum of the electron density irregularities that cause scintillations.

Scintillation usually occurs when the Fresnel dimension of the propagating radio wave is of the order of the scale of irregularity in the ionosphere. Scintillation activities were classified [1] as weak $0.17 \le S_4 \le 0.3$, moderate $0.3 \le S_4 \le 0.5$, and strong $S_4 > 0.5$. Under a weak scattering assumption, only the observed values of the index $S_4 > 0.3$ were used; the values $S_4 > 0.3$ up to 0.45 were recorded by the GPS satellites. For very weak scintillations, $S_4 < 0.2$. For low latitudes, the scintillation easily reaches the strong regime ($S_4 > 0.7$).

We use a "hybrid" spectral function of electron density irregularities containing both anisotropic Gaussian and power-law spectra [7]

$$V_n(\mathbf{k}) = A_p\sigma_n^2\frac{l_\parallel^3}{\chi^2}\frac{1}{\left[1+l_\perp^2(k_x^2+k_y^2)+l_\parallel^2k_z^2\right]^{p/2}}\exp\Big(-\frac{k_x^2l_\parallel^2}{4\chi^2}-p_1\frac{k_y^2l_\parallel^2}{4}-p_2\frac{k_z^2l_\parallel^2}{4}-p_3k_yk_zl_\parallel^2\Big), \quad (3.1)$$

where

$$p_1=(\sin^2\gamma_0+\chi^2\cos^2\gamma_0)^{-1}\left[1+(\chi^2-1)^2\sin^2\gamma_0\cos^2\gamma_0/\chi^2\right], \quad p_2=(\sin^2\gamma_0+\chi^2\cos^2\gamma_0)/\chi^2,$$
$$p_3=(\chi^2-1)\sin\gamma_0\cos\gamma_0/2\chi^2;\ A_p=\Gamma\Big(\frac{p}{2}\Big)\Gamma\Big(\frac{5-p}{2}\Big)\sin\Big(\frac{p-3}{2}\pi\Big),$$

$\Gamma(x)$ is the gamma function. The anisotropy factor $\chi = l_\parallel/l_\perp$ is the axial ratio of the longitudinal and transverse characteristic linear scales of elongated ionospheric irregularities, γ_0 is the inclination angle of extended ionospheric irregularities with respect to the geomagnetic field, σ_n^2 is the dispersion of electron density turbulence. Anisotropic shape of the ionospheric plasmonic structures is a result of the diffusion processes in the longitudinal and perpendicular to the field directions.

Substituting (3.1) into (2.3), we obtain

$$W_\varphi(\eta_x,\eta_y,L)=\frac{\pi^{3/2}}{2}\sigma_n^2\frac{\xi^3k_0L}{\chi^2}\int\limits_{-\infty}^{\infty}dx\int\limits_{-\infty}^{\infty}dy\ \frac{e_0^2+e_1^2}{(B_0+B_1)^{1.25}}$$
$$\times\exp\Big[-\frac{\xi^2}{4}(D_0x^4+D_1x^3+D_2x^2+D_3x+D_4)\Big]\exp(-i\eta_xx-i\eta_yy), \quad (3.2)$$

where

$$\xi=k_0l_\parallel, \quad B_0=1+\frac{\xi^2}{\chi^2}y^2+\frac{\xi^2}{16}h_2^2, \quad e_0=2d_1+(G''d_0+G'd_1)x, \quad e_1=2d_0+(G'd_0-G''d_1)x,$$
$$B_1=\xi^2\left\{\frac{1}{16}(h_0^2x^4+2h_0h_1x^3)+\left[\frac{1}{\chi^2}+\frac{1}{16}(h_1^2+2h_0h_2)\right]x^2+\frac{\xi^2}{8}h_1h_2x\right\},$$
$$D_0=\frac{p_2}{16}h_0^2, \quad D_1=\frac{p_2}{8}h_0h_1, \quad D_2=\frac{1}{\chi^2}+\frac{p_2}{16}h_1^2+\frac{p_2}{8}h_0h_2+p_3yh_0,$$
$$D_3=\frac{p_2}{8}h_1h_2+p_3yh_1, \quad D_4=p_1y^2+\frac{p_2}{16}h_2^2+p_3yh_2.$$

The variance of the phase fluctuations for $\eta_x=\eta_y=0$ can be written as

$$\langle\varphi_1^2\rangle=\frac{\pi^{3/2}}{2}\sigma_n^2\frac{\xi^3k_0L}{\chi^2}\int\limits_{-\infty}^{\infty}dx\int\limits_{-\infty}^{\infty}dy\ (A_1+iA_2)V_n\left[k_0x,k_0y,-k_0(\Phi_2+i\Phi_1)\right], \quad (3.3)$$

where

$$A_1=4(d_0^2+d_1^2)-(\alpha_1^2+\alpha_2^2)x^2, \quad A_2=2(4d_0d_1-\alpha_1\alpha_2x^2),$$
$$\Phi_1=\frac{1}{4}(\mathrm{g}_1x^2-\mathrm{g}_2x), \quad \Phi_2=(\mathrm{g}_3x^2+\mathrm{g}_4x+\mathrm{g}_5)/4,$$
$$\mathrm{g}_1=(P'G''+P''G')y, \quad \mathrm{g}_2=G''y^2-2(G''+P''\mu), \quad \mathrm{g}_3=(G''P''-G'P')y,$$
$$\mathrm{g}_4=G'y^2+2(G'-P'\mu), \quad \mathrm{g}_5=4\mu, \quad \alpha_1=G''d_0+G'd_1, \quad \alpha_2=G'd_0-G''d_1.$$

Substituting (3.2) into equation (3.3), we obtain

$$\langle\varphi_1^2\rangle=\frac{\pi^{3/2}}{2}\sigma_n^2\frac{\xi^3k_0L}{\chi^2}\int\limits_{-\infty}^{\infty}dx\int\limits_{-\infty}^{\infty}dy\ \frac{1}{\Lambda_3^2+\Lambda_4^2}$$
$$\times\left[(A_1\Lambda_3+A_2\Lambda_4)+i(A_2\Lambda_3-A_1\Lambda_4)\right]\exp\left(-\frac{\xi^2}{4}J_0+i\frac{\xi^2}{4}J_1\right),$$

where

$$\Lambda_1 = \mathrm{g}_1\mathrm{g}_3x^4 + (\mathrm{g}_1\mathrm{g}_4 - \mathrm{g}_2\mathrm{g}_3)x^3 + (\mathrm{g}_1\mathrm{g}_5 - \mathrm{g}_2\mathrm{g}_4)x^2 - \mathrm{g}_2\mathrm{g}_5x,$$

$$\Lambda_2 = 1 + \frac{\xi^2}{\chi^2}y^2 + \frac{\xi^2}{16}\Bigg[(\mathrm{g}_3^2 - \mathrm{g}_1^2)x^4 + 2(\mathrm{g}_1\mathrm{g}_2 + \mathrm{g}_3\mathrm{g}_4)x^3 + \left(\mathrm{g}_4^2 - \mathrm{g}_2^2 + 2\mathrm{g}_3\mathrm{g}_5 + \frac{16}{\chi^2}\right)x^2 + 2\mathrm{g}_4\mathrm{g}_5x + \mathrm{g}_5^2\Bigg],$$

$$\Lambda_3 = \Lambda_2^2 - \frac{\xi^4}{64}\Lambda_1,\ \Lambda_4 = \frac{\xi^2}{4}\Lambda_1\Lambda_2,\ J_1 = \frac{p_2}{8}\Lambda_1 - 4p_3y\Phi_1,$$

$$J_0 = p_1y^2 - 4p_3y\Phi_2 + \frac{p_2}{16}\Bigg[(\mathrm{g}_3^2 - \mathrm{g}_1^2)x^4 + 2(\mathrm{g}_1\mathrm{g}_2 + \mathrm{g}_3\mathrm{g}_4)x^3 + \left(\mathrm{g}_4^2 - \mathrm{g}_2^2 + 2\mathrm{g}_3\mathrm{g}_5 + \frac{16}{p_2\chi^2}\right)x^2 + 2\mathrm{g}_4\mathrm{g}_5x + \mathrm{g}_5^2\Bigg].$$

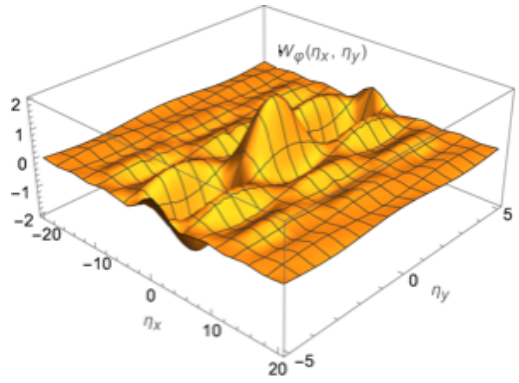

FIGURE 1. Correlation function of the phase fluctuations.

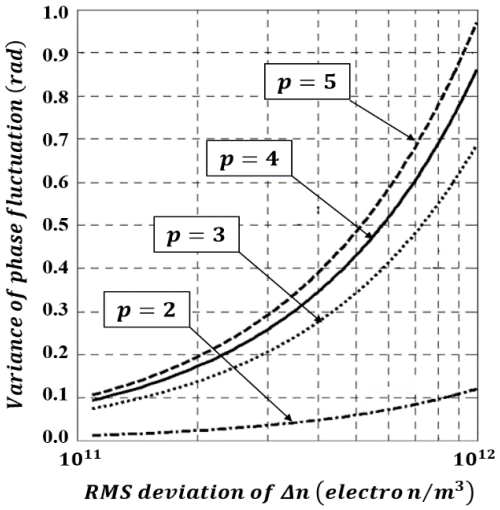

FIGURE 2. Root-mean-square (RMS) deviation of the phase fluctuations for different power-law spectral index p.

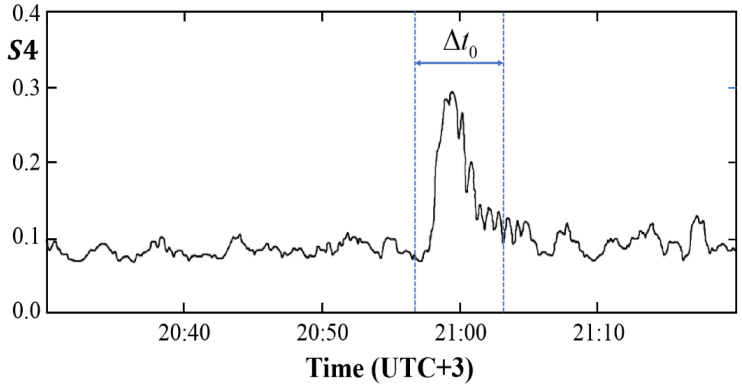

FIGURE 3. Monitoring of the scintillation index S_4 for different observation time intervals.

Figure 1 shows the random phase correlation function as a function of distances η_x and η_y between the observation points. Unlike the polar ionosphere, in the equatorial region this function oscillates in the valley due to scintillations.

Figure 2 illustrates the dependence of randomly varying phase variance on the root-mean-square deviation of electron density fluctuations for different spectral index p. The power-law spectral index p of the phase correlation function is associated with the scintillation index. For weak and moderate scintillations, spectral index p varies in the interval $1.4 - 2.6$. Numerical calculations are carried out by using the experimental data at $p = 1.5$.

Figure 3 illustrates mainly weak temporal variations of the scintillation index $S_4 = 0.7 - 0.3$ for different observation time intervals. Scintillation level reaching its maximum value at night: 21:00 hour, then gradually decreases. Frequency of the navigation satellite PRN2 GPS SRNS signal is about 1 GHz.

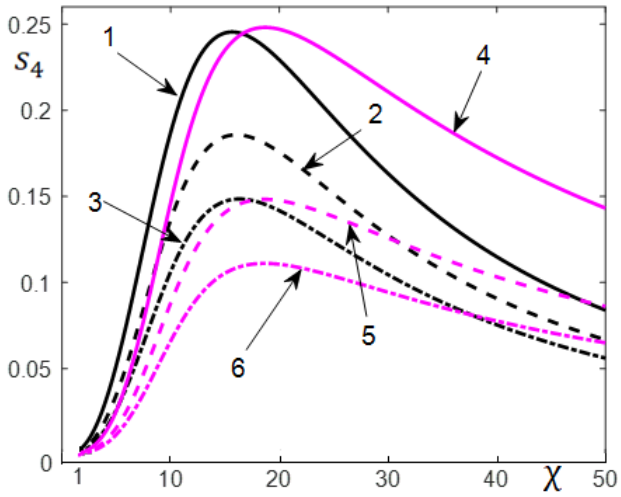

FIGURE 4. Scintillation index versus anisotropy factor of elongated electron density irregularities.

Figure 4 illustrates the dependence of the weak scintillation index S_4 on the anisotropy parameter χ of extended irregularities for different slope angle γ_0 for weak and moderate scintillations in the equatorial ionosphere. Black curves correspond to the O- wave, purple curves to the E- waves. Curves 1 and 4 relate to the tilt angle γ_0°, curves 2 and 5– to the tilt angle $\gamma_0 = 10^\circ$, and curves 3 and 6 to the tilt angle $\gamma_0 = 30^\circ$.The maximum of the S_4 curves related to the O-wave, is shifted to the

right $\chi = 15.66 - 16.4$; the maximum relating to the E-wave is shifted to the left in the interval $\chi = 18.7 - 18.5$.

4. Conclusion

This paper examines the influence of ionospheric scintillations caused by RSD of the electron density fluctuations in the equatorial ionosphere on the phase fluctuation of the navigation radio signal. Polarization coefficients and the second order statistical moments of scattered RWs are calculated analytically for the first time. Analytical calculations are performd by using the Wentzel–Kramers–Brillouin method for small-scale electron density irregularities. The correlation function of the phase fluctuations is obtained for an arbitrary MCF of electron density fluctuations containing complex permittivity and conductivities (Hall, Pedersen and longitudinal) of the equatorial ionosphere for both O- and E- waves, as well as anisotropy parameters characterizing elongated electron density irregularities. Using the experimental observations of the GNSS radiating radio signals with the frequency 1GHz, new features of the "Fontan Effect" in the equatorial ionosphere are revealed. The crests occur at the geomagnetic equator corresponding to the O- and E- waves. Using the experimental data, the spectral index of the "hybrid" power-law spectrum of electron density fluctuations is applied. GPS observation data are analyzed. It is shown that weak and moderate scintillations arise in the equatorial ionosphere during the propagation of radio signals through small-scale electron density irregularities. A new feature of the "Fountain Effect" in the equatorial ionosphere at weak and moderate scintillations is discovered due to the parameters of anisotropy of electron density fluctuations. The angle of inclination of elongated electron density irregularities shifts maxima of the O- and E- waves in the opposite directions.

Investigation of the scintillation effects and ionospheric irregularities is an actual problem for the propagation of electromagnetic waves in the terrestrial ionosphere, plasma turbulence, development and application of observation systems.

The obtained results are quite encouraging. Indeed, one of the deficiencies of the scintillation theory is the vague link between the observable scintillation parameters and the physics of the processes that are responsible for producing the irregularities in conducting polar ionosphere. The general morphology of ionospheric scintillation is reasonably well known. The results presented in this paper suggest that a careful study of the scintillation statistics might reveal some new insight into the mechanisms that are involved. The obtained results will have wide applications both in natural and in laboratory plasmas.

Acknowledgement

This research was funded by the Shota Rustaveli National Science Foundation of Georgia (SRNSFG), grant NFR-21-316 "Investigation of the statistical characteristics of scattered electromagnetic waves in the terrestrial atmosphere and application". The Second author was partially supported by European Commission HORIZON EUROPE WIDERA-2021-ACCESS-03 Grant Project GAIN (grant agreement no.101078950).

References

1. L. Alfonsi, A. W. Wernik, M. Materassi, L. Spogli, Modelling ionospheric scintillation under the crest of the equatorial anomaly. *Advances in Space Research* **60** (2017), no. 8, 1698–1707.
2. M. Aydogdu, E. Guzel, A. Yesil, O. Ozcan, M. Canyilmaz, Comparison of the calculated absorption and the measured field strength of HF waves reflected from the ionosphere. *Il Nuovo Cimento* **30** (2007), no. 3, 243–253.
3. Santimay Basu, Sunanda Basu, Equatorial scintillations–a review. *Journal of Atmospheric and Terrestrial Physics* **43** (1981), no. 5-6, 473–489.
4. B. N. Gershman, L. M. Erukhimov, Yu. Ya. Yashin, *Wave phenomena in the Ionosphere and Space Plasma*. Nauka, Moscow, 1984.
5. A. Ishimaru, *Wave Propagation and Scattering in Random Media*. Reprint of the 1978 original. With a foreword by Gary S. Brown. IEEE/OUP Series on Electromagnetic Wave Theory. An IEEE/OUP Classic Reissue. IEEE Press, New York, 1997.
6. G. Jandieri, A. Ishimaru, B. Rawat, V. Gavrilenko, O. Kharshiladze, Statistical moments and scintillation level of scattered electromagnetic waves in the magnetized plasma. *PIER C* **84** (2018), 11–22.

7. G. Jandieri, A. Ishimaru, B. Rawat, O. Kharshiladze, Zh. Diasamidze, Power spectra of ionospheric scintillations. *Advanced Electromagnetics* **6** (2017), no. 4, 42–51.
8. G. Jandieri, A. Ishimaru, V. G. Gavrilenko, N. Mchedlishvili, O. Kharshiladze, Power spectra of radio waves scintillation in the high-latitude conductive terrestrial ionosphere. *Bulletin of TICMI* **27** (2023), no. 2, 81–94.
9. G. Jandieri, N. Tugushi, Statistical characteristics of the temporal spectrum of scattered radiation in the equatorial ionosphere. *Journal of Environmental and Earth Sciences* **5** (2023), no. 1, 85–94.
10. G. Jandieri, N. Tugushi, Transformation of the spatial spectrum of scattered radio waves in the conductive equatorial ionosphere. *Electronics* **12** (2023), no. 13, 1–11.
11. T. Maruyama, Ionospheric irregularities. *Journal of the Communications Research Laboratory* **49** (2002), no. 3, 163–179.
12. J. P. McClure, W. B. Hanson, J. H. Hoffman, Plasma bubbles and irregularities in the equatorial ionosphere. *Journal of Geophysical Research* **82** (1977), no. 19, 2650–2656.
13. K. Patel, Ashutosh K. Singh, P. Subrahmanyam, A. K. Singh, Modeling of ionospheric scintillation at low-latitude. *Advances in Space Research* **47** (2011), no. 3, 515–524.
14. C. L. Rufenach, Power-law wave number spectrum deduced from ionospheric scintillation observations. *Journal of Geophysical Research* **77** (1972), no. 25, 4761–4772.
15. R. F. Woodman, C. La Hoz, Radar observations of F region equatorial irregularities. *Journal of Geophysical Research* **81** (1976), no. 31, 5447–5466.

(Received 19.04.2024)

[1]International Space Agency Georgian Society, Georgian Technical University, 77 Kostava Str., Tbilisi 0171, Georgia

[2]Muskhelishvili Institute of Computational Mathematics of the Georgian Technical University, 4 Grigol Peradze Str., Tbilisi 0159, Georgia

[3]Department of Control System, Georgian Technical University, 77 Kostava Str., Tbilisi 0171, Georgia
Email address: george.jandieri@gtu.ge
Email address: z.sanikidze@gtu.ge
Email address: nino.mchedlishvili@gtu.ge